Stokes-Einstein violation for liquids with bounded potentials

H.-O. May*
University of Applied Sciences, Darmstadt, Germany

P. Mausbach
University of Applied Sciences, Cologne, Germany

(Received 2 March 2007; revised manuscript received 30 June 2007; published 14 September 2007)

The Stokes-Einstein relation between shear viscosity, diffusion constant, and temperature holds in many liquids, but there are certain examples where the relation fails. In this study, we consider liquids where the interaction potential is bounded, and we find that a different behavior of the Stokes-Einstein relation is possible, where the relation between shear viscosity, diffusion constant, and temperature grows linearly with the viscosity. This special behavior occurs when the potential is bounded and full overlap between the particles is possible. We try to show that the peculiar departure from the classical Stokes-Einstein relation can be explained by this possible overlap of particles by using a hydrodynamic model. Then we compare our result with molecular dynamics simulations for the Gaussian core model liquid.

DOI: 10.1103/PhysRevE.76.031201 PACS number(s): 66.20.+d, 66.10.Cb, 61.20.Gy, 61.20.Ja

I. INTRODUCTION

In 1905 [1] Einstein derived a relation between diffusion constant D, shear viscosity η, and temperature T under the assumption that the diffusing particles are much larger than the molecules comprising the fluid:

$$\frac{D\eta}{T} = S, \tag{1}$$

where S is a constant. He used the Stokes solution for the calculation of the drag force on a sphere. It has been well-established, however, that this relation holds not only for the diffusion of large particles, but also for small particles and even for self-diffusion in many ordinary fluids. The Stokes-Einstein (SE) relation is successfully used for the prediction of the diffusion constant.

There are certain examples where the SE relation fails. Mostly discussed in this context is a variety of fragile glass-forming liquids, where S becomes larger with decreasing temperature as the glass transition is approached [2]. A very common interpretation of the SE breakdown near the glass transition is the assumption of the presence of large dynamic heterogeneities. These spatially heterogeneous dynamical regions are the consequence of highly mobile molecules forming clusters and moving cooperatively, which causes a decoupling of translational diffusion from viscosity [3–8]. In order to explain this observation, Hodgon and Stillinger [9] propose a two-zone and a continuum model, which are based on the fluid flow equations. They receive plausible values for the size of the fluidized region and the mean-field reduction in viscosity.

Very recent measurements on supercooled water confined in nanopores [10] show that the SE relation breaks down well above the glass transition temperature of water calling out for a different scenario. It was speculated [11] that the cause of the SE breakdown in supercooled water is crossing the Widom line, which arises from the liquid-liquid critical point.

Normally unbounded potentials are considered in theoretical studies. A very different situation occurs for liquids with bounded potentials. This leads to new models and scenarios because overlapping between particles is possible. Mausbach and May [12] show some results on the relation between diffusion constant and shear viscosity (see Fig. 1) for the Gaussian core model (GCM) liquid. Bounded potentials, such as in the GCM, have received much attention during the last years [13] because they can be used for modeling systems, such as polymer chains in good solvents, star copolymer suspensions, or micelles in a solvent. As clearly shown in Fig. 1, the SE relation is violated. Here, $D'\eta'/T'$ is shown

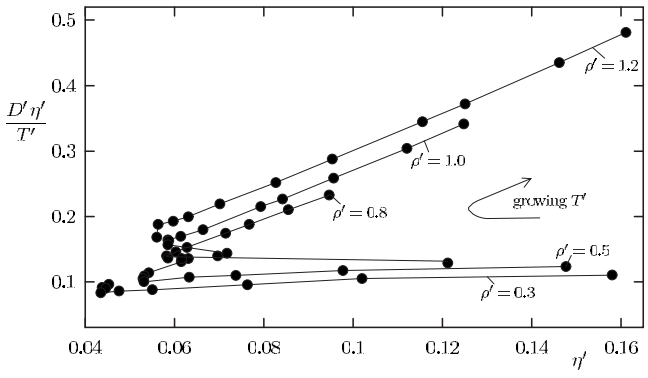

FIG. 1. Results of molecular dynamics simulations for the Gaussian core model liquid: $\frac{D'\eta'}{T'}$ is shown as function of the shear viscosity η', where the density is constant at each curve; T' varies from 0.006 to 0.08 for $\rho'=0.3$, and from 0.002 to 0.08 for $\rho'=1.2$ as indicated by the arrow; D', η', T', and ρ' are dimensionless quantities [see Eq. (17)]. The domain, where $\frac{D'\eta'}{T'}$ is nearly independent of η', characterizes classical Stokes-Einstein behavior. The domain with linear viscosity dependence indicates the different behavior where the influence of overlapping particles becomes dominant. For isochors between $\rho'=0.3$ and 1.2 a distinguished crossover between these two domains is present.

*helge-otmar_may@web.de

as a function of the shear viscosity η', where the density is constant at each curve. D', η', and T' are dimensionless quantities [see Eq. (17)]. Obviously, there are two different domains for each curve. One domain is nearly independent of η', indicating that the SE relation is valid (we will refer to it as the "classic" branch in the following). In the other domain, S' grows linearly with η', where the SE relation is violated (the "nonclassic" branch). It was already shown in [14–18] that special attributes of the GCM liquid are responsible for many anomalies of thermodynamic and transport properties.

We will try to show in the following that this peculiar slope of $D'\eta'/T'$ can be explained by the possible overlap of particles. For this we use the same assumption as for the proof of the classical SE relation, and we find an equation for $D'\eta'/T'$ growing linearly with the viscosity.

II. HYDRODYNAMIC MODEL

We consider the steady-state fluid flow around a stationary sphere of radius a, where the fluid is moving very slowly around the particle. The linearized Navier-Stokes equation and the equation of continuity are valid for the flow around the sphere:

$$\vec{\nabla} p = \eta \Delta \vec{v}, \tag{2}$$

$$\vec{\nabla} \cdot \vec{v} = 0, \tag{3}$$

p is the pressure (it should be $p \to 0$ if $u \to 0$, u is the velocity far away from the sphere) and $\vec{v}$ is the velocity vector.

Because penetration of particles is possible for fluids with bounded potentials, a flow within the sphere is possible. Within the sphere, we have a resistance which influences the flow, as in the case of a porous medium, and if the flow velocity is small, we can use Darcy's law:

$$\vec{\nabla} p = -\kappa \vec{v}, \tag{4}$$

replacing Eq. (2) within the sphere, where κ is a constant.

In spherical coordinates r, θ, and φ we use the following ansatz [19]:

$$v_r = u f(r) \cos\theta, \quad v_\theta = -u\left(\frac{r}{2} f'(r) + f(r)\right) \sin\theta \tag{5}$$

for Eq. (2) (outer solution), the equation of continuity is automatically fulfilled. If we take the curl of Eq. (2), then we have

$$4f' - 4rf'' - 4r^2 f''' - \frac{1}{2} r^3 f'''' = 0 \tag{6}$$

with the solution

$$f(r) = C_1 + C_2 r^2 + C_3/r + C_4/r^3, \tag{7}$$

where $C_1 = 1$ and $C_2 = 0$ because $f(\infty) = 1$. For the inner solution, we use the same ansatz as before, replacing $f(r)$ by $g(r)$. Then the curl of Eq. (4) yields

$$rg'' + 4g' = 0 \tag{8}$$

with the solution

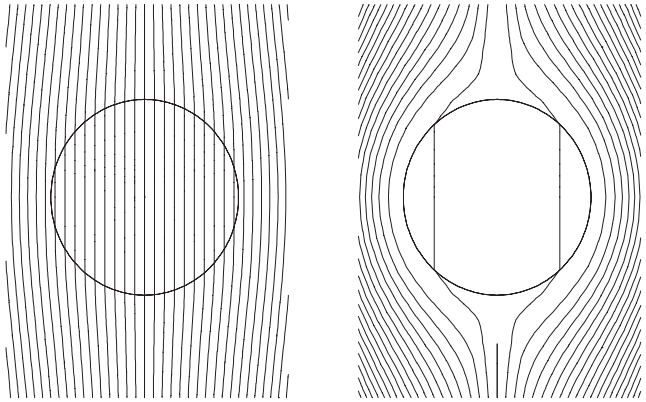

FIG. 2. Streamline pictures of the flow solution: left: small κ $\left(\frac{\kappa a^2}{u\eta} = 1\right)$ and right: large κ $\left(\frac{\kappa a^2}{u\eta} = 100\right)$. Flow direction is from bottom to top.

$$g(r) = D_1 + D_2/r^3. \tag{9}$$

Because the velocity within the sphere must be finite, it is $D_2 = 0$, and therefore the velocity within the sphere is constant. For the remaining three constants D_1, C_3, and C_4, we use the three conditions that the velocity components v_r, v_θ, and the pressure p must be continuous at $r = a$, and we receive

$$C_3 = \frac{-3\kappa a^3}{2\kappa a^2 + 3\eta}, \quad C_4 = \frac{\kappa a^5}{2\kappa a^2 + 3\eta}, \quad D_1 = \frac{3\eta}{2\kappa a^2 + 3\eta}. \tag{10}$$

Integrating now

$$\sigma_{rr} \cos\theta - \sigma_{r\theta} \sin\theta = \cos\theta\left(-p + 2\eta \frac{\partial v_r}{\partial r}\right) - \eta \sin\theta\left(\frac{1}{r}\frac{\partial v_r}{\partial \theta} + \frac{\partial v_\theta}{\partial r} - \frac{v_\theta}{r}\right) \tag{11}$$

over the surface of the sphere at $r = a$ yields the force on the sphere

$$F = 12u \frac{\pi \eta \kappa a^3}{2\kappa a^2 + 3\eta}. \tag{12}$$

If $\kappa = 0$, then there is no resistance, and therefore $F = 0$; if $\kappa \to \infty$, no flow within the sphere is possible, and the famous Stokes formula $F = 6\pi\eta a u$ is valid.

In Fig. 2, streamline pictures of the flow solution are given (flow direction is from bottom to top): The left picture shows the streamlines if κ is small $\left(\frac{\kappa a^2}{u\eta} = 1\right)$. In this case, the parallel flow is only slightly disturbed. The right picture gives the solution for the case of large κ $\left(\frac{\kappa a^2}{u\eta} = 100\right)$, where the streamlines around the sphere are much denser than inside the sphere, indicating that the flow within the sphere is only very slow. The streamlines within the sphere are parallel lines, and the velocity is constant inside. If we denote the flow direction by z, then we have within the sphere

$$\vec{v} = \frac{3\eta u}{2\kappa a^2 + 3\eta}\vec{e}_z, \tag{13}$$

with the unit vector $\vec{e}_z$ in the flow direction.

Following the argumentation of Einstein, the relation between diffusion coefficient and driving force F of suspended particles is given by

$$DF = k_B T u, \tag{14}$$

where u is the particle velocity in the suspension and k_B is Boltzmann's constant. Now we can use Eq. (12) to eliminate F, and we get

$$\frac{D\eta}{T} = k_B \frac{2\kappa a^2 + 3\eta}{12\pi\kappa a^3}. \tag{15}$$

If, again, κ becomes very large, then we have $D\eta/T = k_B/(6\pi a) = \text{const}$.

III. APPLICATION ON THE GCM FLUID

To verify these formulas, we compare the results of our hydrodynamic model with molecular dynamics (MD) simulations for a liquid with a bounded potential. One of the most discussed potentials, in this context, is the GCM:

$$\Phi(r) = \Phi_0 \exp[-(r/\sigma)^2]. \tag{16}$$

Φ_0 and σ are the height and width of the interaction profile and are units of energy and length; r is the distance between two particles. We introduce dimensionless variables: m is the mass of a particle, then r', η', T', D', and κ' are dimensionless quantities with

$$r = \sigma r', \quad \eta = \frac{\sqrt{m\Phi_0}}{\sigma^2}\eta', \quad k_B T = \Phi_0 T',$$

$$D = \sigma\sqrt{\frac{\Phi_0}{m}}D', \quad \kappa = \frac{\sqrt{m\Phi_0}}{\sigma^2}\kappa', \tag{17}$$

and we get in dimensionless variables, similar to Eq. (15):

$$\frac{D'\eta'}{T'} = \frac{1}{6\pi a'} + \frac{1}{4\pi\kappa' a'^3}\eta'. \tag{18}$$

In a very intensive study [18], we analyzed the GCM system with high resolution in an extended phase space. We used MD simulations, where the equations of motion were integrated via the leap frog algorithm. The systems consisted of $N=864$ particles, and the interactions were cut off at a dimensionless distance of $r'_C=3.2$. The simulations covered isochors of dimensionless densities ($\rho' = N\sigma^3/L_B^3$, L_B is the edge length of the periodic box) from $\rho'=0.1$ to 2.0 and dimensionless temperatures in a range from $T'=0.002$ to 0.08. In this study, we used production periods up to 800 000 time steps.

For the calculation of the self-diffusion coefficient (SDC) and the shear viscosity, we applied the Green-Kubo formula, based on the integrated velocity and pressure tensor autocorrelation function, respectively. From these simulation series, we received very precise data for structural and thermodynamic properties, as well as for the SDC D'; but, as a well-known problem, the viscosity data were covered with strong statistical noise [17].

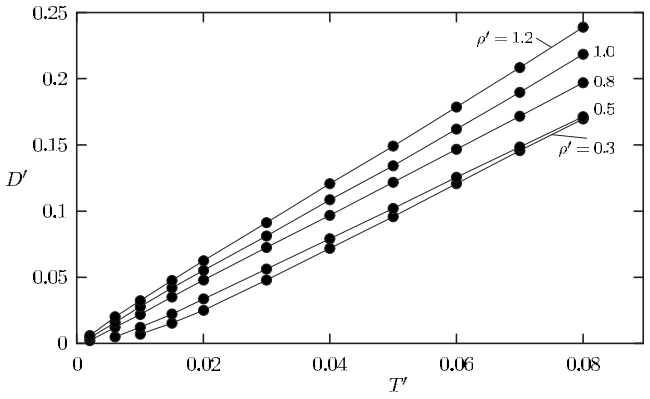

FIG. 3. Temperature dependence of the self-diffusion coefficient D' along various isochors ranging from $\rho'=0.3$ to 1.2. The diffusion coefficient grows monotonically with increasing temperature.

Therefore we recalculated the SDC and the viscosity for densities of $\rho'=0.3$, 0.5, 0.8, 1.0, and 1.2, where systems with $N=2048$ particles and production periods of 10×10^6 time steps were used. The simulated temperatures were $T'=0.002$, 0.006, 0.01, and 0.015, and $T'=0.02$ to 0.08 in steps of 0.01. All other parameters were the same as described in [18].

In Fig. 3, the temperature dependence of the SDC D', for the five isochores at $\rho'=0.3$, 0.5, 0.8, 1.0, and 1.2, is given. In general, the SDC grows with increasing temperature, and in the density range shown in Fig. 3 an anomalous increase of D', upon increasing density, is observed. A discussion of these phenomena can be found in [18].

Figure 4 shows the temperature dependence of the shear viscosity for the five isochors. Five small thick lines are added at the bottom of Fig. 4, indicating the approximate freezing temperature at $\rho'=0.3$, 0.5, 0.8, 1.0, and 1.2 from right to left. In Fig. 4, up to a density of $\rho'\approx0.8$, the shear viscosity rises sharply in the region of the transition to the solid state because the approach to this phase boundary causes a noticeable tail in the pressure tensor autocorrelation function. When the temperature is increased from the solidification temperature at constant density, the shear viscosity passes through a minimum, followed by a further increase. The strong negative gradient of the shear viscosity at low temperatures disappears when the density is further increased, as for $\rho'=1.0$ and especially for $\rho'=1.2$, because the freezing temperature converges to zero in the high-density limit [14,15]. In this region, where reentrant melting occurs, the system remains fluid at all densities [15,20–22].

Using the transport properties from Figs. 3 and 4, the relation $D'\eta'/T'=S'$ in Fig. 1 is plotted against η' for isochoric curves of densities ranging from $\rho'=0.3$ to 1.2. The temperature raises from $T'=0.006$ to 0.08 for $\rho'=0.3$ and from $T'=0.002$ to 0.08 for $\rho'=1.2$, as indicated by the arrow in Fig. 1.

In Fig. 1, we have to distinguish two different branches of each curve. On the classic part, $D'\eta'/T'$ is nearly constant,

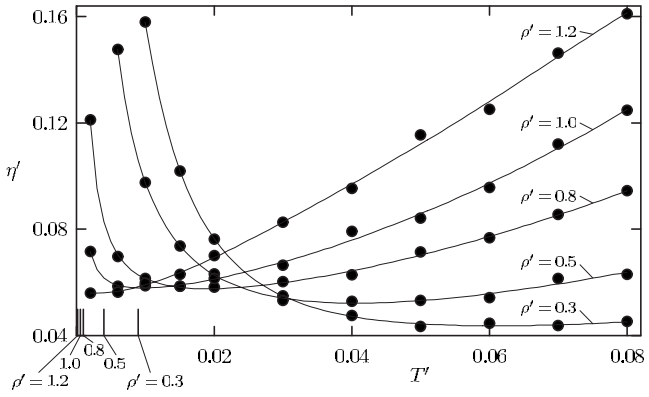

FIG. 4. Temperature dependence of the shear viscosity η' along various isochors ranging from $\rho'=0.3$ to 1.2. The shear viscosity rises sharply in the region of the transition to the solid state. The approximate location of the freezing temperature for the different densities is indicated as small thick lines at the left bottom of the figure. The viscosity isochors for densities between $\rho'=0.3$ and 1.0 drop sharply when the temperature increases and pass through a minimum, followed by an increase of η' upon further heating. The strong increase of the viscosity near the freezing point is reduced when the system is compressed. In this region of the phase space reentrant melting of the GCM system occurs. At a density of $\rho'=1.2$, the freezing temperature approximates to zero and the shear viscosity grows monotonically with increasing temperature in the range we have simulated.

which means that the influence of overlapping is low. On the nonclassic part, where $D'\eta'/T'$ grows linearly with η' as in Eq. (18), the influence of overlapping is dominant. This is in agreement with the finding of [18]: When the density becomes higher, overlapping of particles becomes more and more important. At low densities (up to $\rho'\cong 0.3$), there is nearly no influence of overlapping. At high density ($\rho'=1.2$), there is only a nonclassic branch. Obviously, for densities between these values both branches exist.

It is not self-evident that κ' and a' must be constant values because it is imaginable that the configuration of the structure through which the particles are moving depends at least on the density. When we consider Eq. (18), then Fig. 1 implies that $\frac{1}{6\pi a'}$ depends slightly on the density; but it seems as if the gradients of the nonclassic branches are nearly constant. From these gradients, we can estimate a value for the resistant constant and we receive

$$\kappa' a'^3 \approx 0.028. \tag{19}$$

IV. CONCLUSION

In this study, we applied the SE approach extended to liquids, where the potential is bounded and where, therefore, overlap between particles is possible. We find that a different behavior of the SE relation is possible, where S grows linearly with the viscosity η. This hydrodynamical model will, of course, not be able to describe all details of overlapping effects because we used a rather simple ansatz with a constant resistant coefficient and a constant diffusion radius, which cannot be expected for all situations. Relation (4) could be replaced by a nonlinear relation, but this would not match the linearized flow equations. Obviously, the hydrodynamical model describes an essential difference between the behavior of penetrating and nonpenetrating particles, and the model is independent of a special potential.

We compared our theory with MD simulations on GCM particles. Penetration is possible for soft matter particles built up from several thousands of atoms or molecules. The GCM can be used as an "effective" potential for such a soft matter system. Having in mind that the theoretical approach uses the picture of large diffusing particles, relation (18) obviously holds for the self-diffusion coefficient D, which was taken from MD simulations. The hydrodynamical model parameters will at least depend on the density of the system as can be expected from the simulation results. It would be interesting to see if relation (18) holds for other bounded potentials.

ACKNOWLEDGMENTS

The simulations presented in this study were conducted at the RUBENS cluster at the University of Siegen. We want to thank Michael Weitzel and Roland Reichardt for substantial support when using the cluster.

[1] A. Einstein, Ann. Phys. **322**, 549 (1905).
[2] P. G. Debenedetti and F. H. Stillinger, Nature (London) **410**, 259 (2001).
[3] J.-L. Barrat, J.-N. Roux, and J.-P. Hansen, Chem. Phys. **149**, 197 (1990).
[4] F. Fujara, B. Geil, H. Sillescu, and G. Fleischer, Z. Phys. B: Condens. Matter **88**, 195 (1992).
[5] M. T. Cicerone, F. R. Blackburn, and M. D. Ediger, J. Chem. Phys. **102**, 471 (1995).
[6] G. Tarjus and D. Kivelson, J. Chem. Phys. **103**, 3071 (1995).
[7] M. D. Ediger, Annu. Rev. Phys. Chem. **51**, 99 (2000).
[8] L. Berthier, Phys. Rev. E **69**, 020201(R) (2004).
[9] J. A. Hodgdon and F. H. Stillinger, Phys. Rev. E **48**, 207 (1993).
[10] S.-H. Chen, F. Mallamace, C.-Y. Mou, M. Broccio, C. Corsaro, A. Faraone, and L. Liu, Proc. Natl. Acad. Sci. U.S.A. **103**, 12974 (2006).
[11] P. Kumar, Proc. Natl. Acad. Sci. U.S.A. **103**, 12955 (2006).
[12] P. Mausbach and H.-O. May, *16th Symposium on Thermophysical Properties*, Boulder, CO, July 30–August 4 (NIST, Boulder, CO, 2006).
[13] C. N. Likos, Phys. Rep. **348**, 267 (2001).
[14] F. H. Stillinger and D. K. Stillinger, Physica A **244**, 358 (1997).
[15] A. Lang, C. N. Likos, M. Watzlawek, and H. Löwen, J. Phys.: Condens. Matter **12**, 5087 (2000).

[16] P. Mausbach and H.-O. May, Proc. Appl. Math. Mech. **5**, 685 (2005).
[17] P. Mausbach and H.-O. May, Proc. Appl. Math. Mech. **6**, 571 (2006).
[18] P. Mausbach and H.-O. May, Fluid Phase Equilib. **249**, 17 (2006).
[19] A. Sommerfeld, *Lectures on Theoretical Physics* (Academic, New York, 1950), Vol. 2.
[20] F. H. Stillinger, J. Chem. Phys. **65**, 3968 (1976).
[21] P. V. Giaquinta and F. Saija, ChemPhysChem **6**, 1768 (2005).
[22] S. Prestipino, F. Saija, and P.V. Giaquinta, Phys. Rev. E **71**, 050102(R) (2005).